21st Australasian Fluid Mechanics Conference
Adelaide, Australia
10-13 December 2018

Three-dimensional measurements of particle clusters at the exit of a turbulent pipe jet

T. C. W Lau[1], J. H. Frank[2] and G. J. Nathan[1]

[1]Centre for Energy Technology, School of Mechanical Engineering
The University of Adelaide, SA 5005, Australia

[2]Combustion Research Facility
Sandia National Laboratories, Livermore, CA 94550, United States

Abstract

An investigation into the phenomenon of particle clustering at the exit of a turbulent two-phase pipe flow was conducted utilising detailed time-resolved tomographic-PIV measurements in conjunction with Voronoi analysis. The flow consisted of an air jet laden with solid, spherical particles, issuing from a long round pipe into a weak co-flow. The pipe diameter was $D =$ 6.22mm, while the pipe length-to-diameter ratio was L/D=160. The jet Reynolds number, based on the pipe diameter, was fixed at $Re_D = 10,000$. Two different particle diameters were investigated, namely $d_p = 0.3$ and 10μm. The corresponding Stokes numbers, based on the large-eddy time-scale, was Sk_D = 0.004 and 1.4, respectively. The particle bulk concentration was ≈190particles/mm^3, which was sufficiently large to result in significant particle-fluid interaction (that is, the flow was in the two-way coupling regime). The results show that for the Sk_D = 1.4 case, particle clustering is significant, with the clusters characterised by their filament or rope-like morphology and their coherence in time. Importantly, they are also detected right from the exit plane, which implies that these clusters were generated inside the pipe. For the case Sk_D = 0.004 particle clustering is negligible, and where detected, clusters tended to be small and incoherent in time, suggesting that they most likely arise out of random motion of individual particles.

Introduction

Particle-laden flows, typically consisting of solid or liquid particles suspended in a fluid, are an important class of flow due to their wide relevance in many natural, scientific and industrial systems. In particular, particle-laden turbulent jets utilising solid particles are commonly employed in industrial systems such as in solid fuel combustion, minerals processing, and, more recently, concentrated solar thermal receivers. In these processes, the instantaneous distributions of particle concentrations can significantly impact chemistry, temperature distributions, heat transfer, particle attrition, emissions and overall process efficiency [1, 14]. However, studies have shown that the phenomenon of particle clustering, whereby particles are instantaneously preferentially concentrated in highly localised regions of the flow, can occur in a wide array of particle-laden flows, including shear flows [5] and turbulent jets [8, 7, 9, 11]. This phenomenon results in highly non-uniform particle distributions within the flow, which in turn impacts the performance of systems employing particle-laden flows. Hence, there is a strong need to improve current understanding of particle clustering in particle-laden turbulent flows.

Complete understanding of particle-laden turbulent flows requires fully-resolved measurements and/or calculations of the velocities of both the discrete (i.e. particle) and gas phases together with particle positions simultaneously in four dimensions (4D, consisting of 3 spatial and 1 temporal). To the authors' knowledge, no such experimental measurements exist for turbulent flows in the regime where particle-fluid interaction are significant (i.e., in the two-way or four-way coupling regime), partly due to the significant practical challenges of obtaining accurate measurements under these conditions. Furthermore, numerical simulations of these flows where both phases are computed directly remains computationally expensive, with almost all computational fluid dynamics (CFD) studies of particle-laden turbulent flows utilising simplifications or models. However, the development of accurate two-phase CFD models is currently hindered by the paucity of detailed experimental measurements under well-characterised conditions that is suitable for model validation.

This paper forms part of a larger research study that aims to advance current understanding of particle-laden flows and particle clustering utilising detailed 4D experimental measurements at the exit of a turbulent particle-laden jet. In particular, this paper aims to demonstrate a method to measure particle clusters and subsequently describe the 3D particle cluster morphology at the turbulent jet exit in the two-way coupling regime. These aims will be met utilising tomographic particle image velocimetry (tomo-PIV) in conjunction with 3D image processing and Voronoi analysis.

Experimental method

The experiment consisted of tomographic-PIV measurements at the exit of a particle-laden turbulent pipe jet, as shown in figure 1. The pipe was a smooth stainless steel round pipe of diameter $D = 6.22$mm and length $L = 1000$mm. The resultant length to diameter ratio of $L/D = 160$ is sufficiently long to result in an approximately fully-developed two-phase pipe flow at the exit [6]. The pipe was mounted vertically such that the flow was opposed to gravity. The jet bulk velocity was fixed at $U_b = 12$m/s, resulting in an exit Reynolds number of $Re_D = \rho_a U_b D/\mu = 10,000$, where ρ_a and μ is the density and dynamic viscosity of air, respectively. A fume hood placed approximately 1m above the pipe exit induced a weak co-flow within the experimental test section, resulting in a jet-to-flow velocity ratio at the exit plane of 12:1.

The pipe jet was laden with two types of spherical particles, namely alumina particles with material density $\rho_p =$ 3950kg/m^3 and mean diameter $d_p \approx 0.5\mu$m, and PMMA particles with material density $\rho_p = 1200$kg/m^3 and mean diameter $d_p = 10\mu$m. The latter particles are mono-disperse, with a standard deviation of particle diameter $\approx 1\mu$m [6]. The resultant exit Stokes numbers for both particles, based on the large-eddy time-scale, were $Sk_D = \rho_p d_p^2 U_b/(18\mu D) = 0.004$ and 1.4, respectively. The bulk particle concentration was fixed at $\Theta_b \approx 190$particles/mm^3, resulting in a volume loading of $\beta = 10^{-4}$ and $\approx 10^{-8}$ for the $d_p = 10\mu$m and 0.5μm particles, respectively. Particles were introduced into the flow at the pipe inlet using a diametrically opposed tee-piece (as shown in figure 1). This inlet condition has previously been shown to assist in achieving symmetric particle distributions at the pipe exit [6].

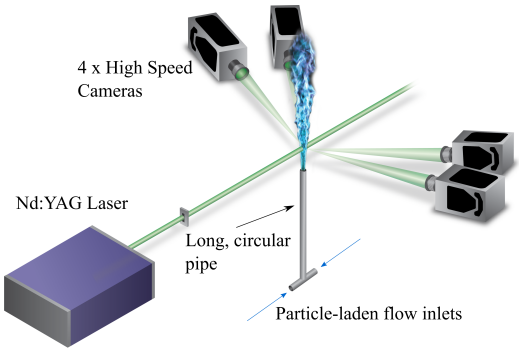

Figure 1: Schematic of the experimental arrangement.

The measurement region was illuminated using a Quantronix Hawk HP dual head laser, operating at a wavelength of 532nm. Each head was operated at a repetition rate of 40kHz, resulting in an overall illumination rate of 80kHz. The laser beam was shaped into a 2.8mm thick light sheet within the imaging region using a series of cylindrical lenses and knife-edge slits. Images of the measurement region were simultaneously recorded using 4 CMOS (Vision Research Phantom v1610) cameras. The viewing angle of the cameras, i.e., the angle between the lens axis and the plane normal to the laser sheet, was $\theta = 20^\circ$, 45°, 135° and 160°, respectively. Each camera utilised a Tamron 180mm f#3.5 1:1 macro lens mounted on a Scheimpflug (tilt-shift) mount. The cameras, which recorded images synchronously with the laser pulses, had an effective array size of $N_{arr} = 512 \times 304$pixels. Images were recorded continuously for 1.345s (resulting in 107,636 images per camera) per experimental run. Each image was corrected for background by subtracting from each image the time-averaged signal recorded without the presence of particles. Calibration measurements for tomographic image registration were conducted before and after each experimental run. This involved recording images of a semi-transparent grid of circular dots at 7 different planes offset from the illumination plane.

Tomographic reconstruction and velocity field calculation

The multiplicative algebraic reconstruction technique (MART) with 5 iterations was used to reconstruct the three-dimensional particle intensity distributions from the images of the 4 cameras. The resultant reconstructed volume corresponded to the region $0 \leq x/D \leq 0.87$ (329 pixels), $-0.95 \leq y/D \leq 0.95$ (713 pixels) and $-0.23 \leq z/D \leq 0.23$ (171 pixels), where x is the axial (streamwise) co-ordinate, y is the co-ordinate parallel to the beam path and z is the co-ordinate normal to the light sheet (depth). The origin is centred on the pipe axis at the exit plane.

The velocity field was computed from successive reconstructed volumes using a multi-pass, multi-grid, fast-Fourier transform algorithm. The final step utilised an interrogation window size of $16 \times 16 \times 16$pixels and an overlap of 75%. Outliers were detected and replaced in a 2 step process. In the first step, outliers were detected using the universal outlier detection method [15] with a $3 \times 3 \times 3$ neighborhood, a threshold value of 2.0 pixels and a normalisation level of 0.1 pixels. Furthermore, vectors were also labeled as outliers if the ratio of the first and second peaks in the correlation plane, $Q < 1.01$. In both these cases, outliers were replaced with interpolated values. The second step, performed after all the reconstructions in the time-series were computed, involved calculating the mean and standard deviation of velocity at each grid location, $\overline{U}$ and σ_U, respectively, and then specifying a vector as an outlier if the velocity was outside the range $\overline{U} - 3\sigma_U \leq U \leq \overline{U} + 3\sigma_U$. These outliers were not interpolated. Instead, the "robust" option of the smoothing method proposed by [4] was used to simultaneously smooth the data and replace these outliers. A low smoothing parameter of $s = 10^{-3}$ was used to avoid over-smoothing the velocity data.

Cluster identification

To reduce tomographic reconstruction artifacts commonly known as "ghost particles", a two-stage scheme was used. In the first stage, ghost particles were detected and removed using the intensity thresholding technique, whereby particle images with a mean intensity below a minimum threshold were removed from further analysis [2]. In the next stage, successive recorded tomographic volume reconstructions were used in conjunction with the measured velocity field to calculate temporally-correlated volumes [13].

Particle positions were measured to sub-pixel accuracy from the temporally-correlated volumes by fitting 3D Gaussian functions to the particle intensity distributions. Clusters were identified from the particle positions using the Voronoi method. This method has previously been demonstrated for two-dimensional measurements [12] but has been extended to three-dimensional measurements in this study. This method firstly involved calculating the vertex co-ordinates of the three-dimensional Voronoi cell and its respective volume, $\forall_v$, for each particle in the reconstructed volume. A Voronoi cell for a particle contains all points that are located closer to that particles than to any other particle. All cells with a normalised volume $\tilde{\forall}_v = \forall_v / \overline{\forall}_v$, larger than a threshold $\tilde{\varepsilon}_v$ were discarded, where $\overline{\forall}_v$ is the mean Voronoi cell volume within the reconstructed image. In this calculation, Voronoi cells with vertices that extend beyond the reconstruction volume were omitted. Clusters were then defined as contiguous groups of three or more Voronoi cells that share an external surface. The threshold $\tilde{\varepsilon}_v$ was calculated by first considering the expected normalised Voronoi volume distribution of a random Poisson process, $\tilde{\forall}_{v,P}$. Since there is no known analytical solution for the probability density function of $\tilde{\forall}_{v,P}$, a curve-fit was chosen using the 3-parameter gamma distribution described by [3]

$$pdf(\tilde{\forall}_v) = c\frac{b^{(a/c)}}{\Gamma(a/c)}\tilde{\forall}_v^{(a-1)} \exp\left(-b\tilde{\forall}_v^c\right). \qquad (1)$$

Here, Γ is the gamma function, while the empirically-derived constants were chosen to be $a = 4.7868$, $b = 4.0681$ and $c = 1.1580$ following [10]. To minimise the detection of particle clusters that were generated through random particle motion, the threshold was selected to exclude 97.5% of the largest (by volume) Voronoi cells expected from a random Poisson process. Mathematically, this threshold is the solution to $cdf(\tilde{\forall}_v) = 0.025$, where $cdf = \gamma(a/c, b\tilde{\forall}_v^c)/\Gamma(a/c)$ is the cumulative distribution function and γ is the lower incomplete gamma function. The value of this threshold was numerically calculated to be $\tilde{\varepsilon}_v = 0.338$. In summary, this methodology identifies as clusters any group of 3 or more particles that are spaced more closely than 97.5% of randomly distributed particles.

Results

Figure 2 presents false-color images of the particle clusters recorded at three successive timesteps for both $Sk_D = 0.004$ and $Sk_D = 1.4$. The results show that for $Sk_D = 0.004$ case, particle clustering is not significant, with nearly no clusters detected in the flow. Importantly, where the clusters are detected, they are small and not coherent in time, which suggests that these regions are not "true" clusters, but are instead regions of temporarily high particle concentration that arise due to random motion of the particles. By contrast, for the $Sk_D = 1.4$ case,

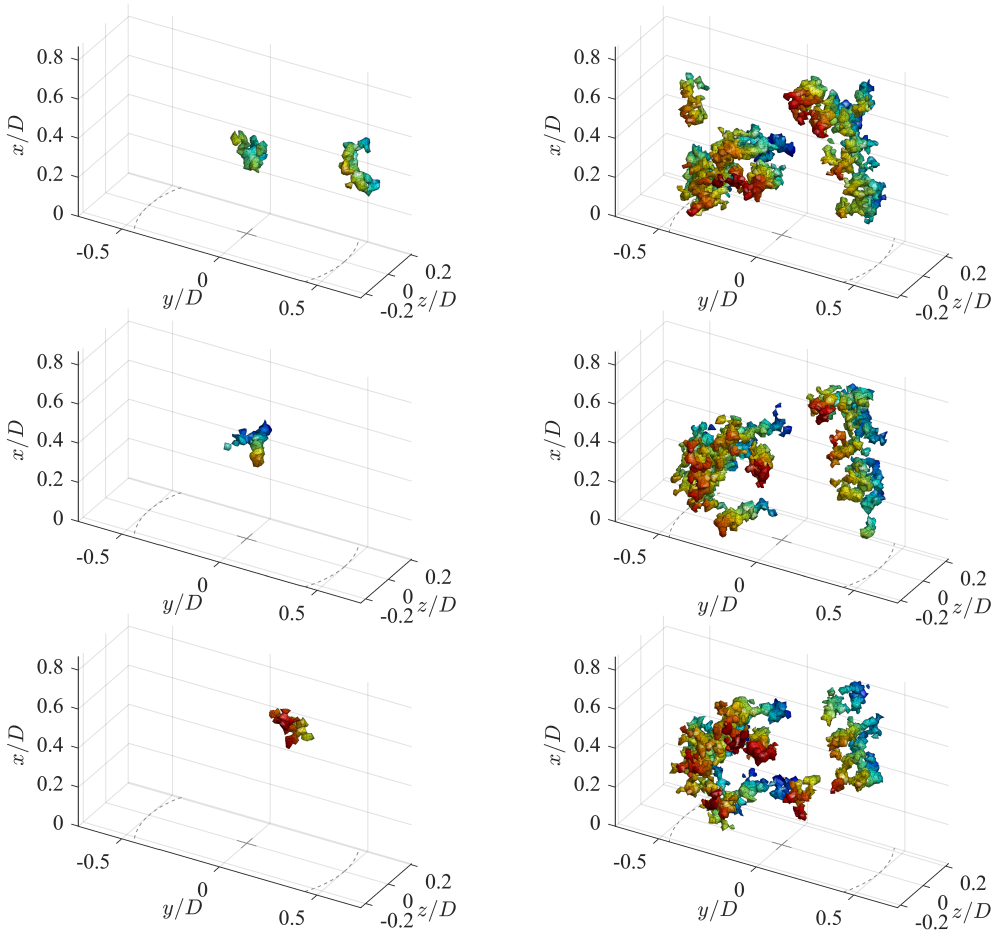

Figure 2: False-color images of particle clusters at the pipe exit for $Sk_D = 0.004$ and $Sk_D = 1.4$, respectively, recorded at 3 successive time-steps. The clusters are colored from red to blue proportional to their depth (z co-ordinate).

particle clustering is significant, consistent with previous studies [9]. Numerous particle clusters of varying size are detected throughout the flow, with the clusters appearing as filament-like or rope-like structures that are coherent in time. Crucially, the clusters are detected right from the exit plane, implying that they are generated inside the pipe.

Figure 3 presents mean (time-averaged) particle concentration $\overline{\Theta}/\Theta_b$, particle cluster probability distribution, $PDF(Clus)$, and the mean particle concentration conditionally-sampled in regions not considered a cluster, $\overline{\Theta}_{Not-Clus}/\Theta_b$, measured at $x/D = 0.5$ for $Sk_D = 1.4$ case. The results show that the mean particle concentration is greater close to the jet edge, consistent with previously published planar data [6] at identical Stokes numbers. However, the peak concentration found in this study, $\overline{\Theta}/\Theta_b \approx 1.4$, is greater than the values of $\overline{\Theta}/\Theta_b \approx 1.2$ found in [6]. This is attributed to differences in Re_D and d_p between both studies. In the case where the data is conditionally-sampled in regions outside of clusters only, the particle mean concentration approaches a more uniform distribution, with a peak concentration of $\overline{\Theta}_{Not-Clus}/\Theta_b \approx 1.05$. Furthermore, the mean particle concentration distribution shows some signs of radial asymmetry, with greater values of $\overline{\Theta}/\Theta_b$ measured at $y/D = 0$, $z/D = \pm 0.5$ than at $y/D = 0.5$, $z/D = 0$. This is possibly due to the effect of the inlets, which were located within the plane $y/D = 0$, suggesting that the 160 pipe diameters of flow development length used in this study was not sufficient to result in a truly fully-developed particle-laden flow at the pipe exit.

Interestingly, the results also show that $PDF(Clus)$ is greater close to the jet edge, i.e., an increase in mean particle concentration is correlated with an increased probability of cluster detection. While this correlation is perhaps not surprising, it is unclear whether particle clustering causes an increase in mean concentration, a greater mean concentration leads to an increased likelihood of particle clusters, or if both phenomenon are coupled. Incidentally, the region close to the jet edge/pipe boundary is the region with the greatest strain rates and turbulence intensities [7]. These results, taken together with the finding that the clusters are likely generated inside the pipe, suggest a link between cluster generation, mean preferential concentration of particles and the flow close the pipe boundary. However, much more work is required to confirm the details of this link.

Conclusions

Detailed 4D measurements of a particle-laden turbulent jet has revealed that for the case where the Stokes number, based on the large-eddy time-scale, is $Sk_D = 1.4$, particle clustering is significant, with the measured particles appearing as filament- or rope-like structures that remain coherent in time within the measurement volume. These clusters were found to be preferentially concentrated close to the jet edge, where the mean

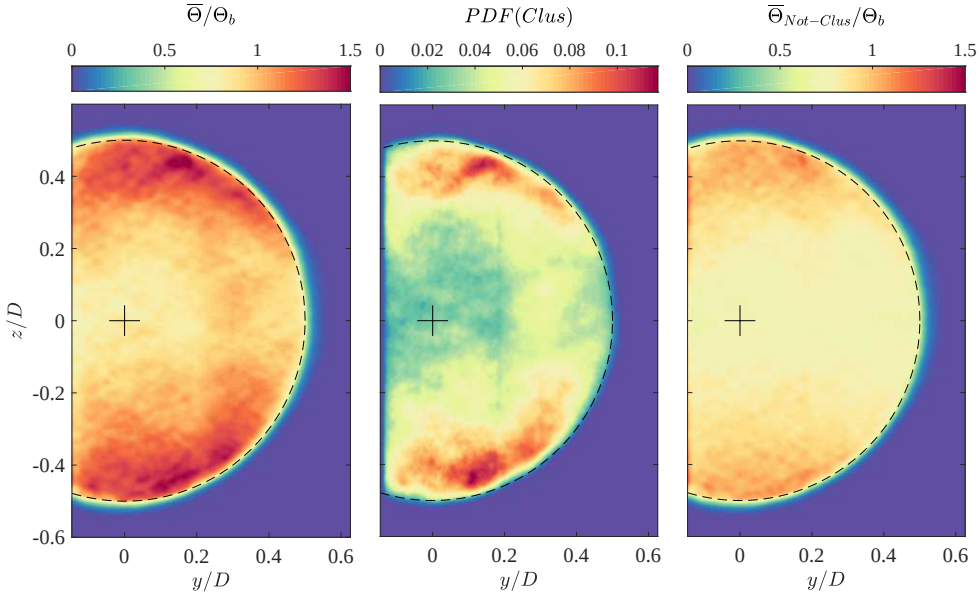

Figure 3: Distributions of normalised mean particle concentration, $\overline{\Theta}/\Theta_b$, probability density of particle clusters, $PDF(Clus)$, and normalised mean concentration conditionally-sampled in regions not identified as clusters, $\overline{\Theta}_{Not-Clus}/\Theta_b$, measured at $x/D = 0.5$ for the case where $Sk_D = 1.4$. Here Θ_b is the bulk particle concentration. The black dashed line indicates the pipe inner diameter, while the "+" symbol denotes the pipe centre.

(time-averaged) particle concentration was also high. Importantly, the results also show that the clusters exist right from the exit plane, implying that particle clusters are generated inside the pipe close to the pipe wall where strain rates and turbulence intensities are expected to be the greatest.

Acknowledgments

The support of the U.S. Department of Energy, Office of Basic Energy Sciences, Division of Chemical Sciences, Geosciences, and Biosciences is gratefully acknowledged. Sandia National Laboratories is a multimission laboratory managed and operated by National Technology and Engineering Solutions of Sandia, LLC., a wholly owned subsidiary of Honeywell International, Inc., for the U.S. Department of Energy's National Nuclear Security Administration under contract DE-NA-0003525. The authors would like to acknowledge the financial contributions of the Australian government through the Australian Research Council (Grant No. DP120102961) and the Australian Renewable Energy Agency (Grant No. USO034).

References

[1] Annamalai, K. and Ryan, W., Interactive processes in gasification and combustion. part 1: Liquid drop arrays and clouds, *Prog. Energy Combust. Sci.*, **18**, 1992, 221–295.

[2] de Silva, C. M., Baidya, R. and Marusic, I., Enhancing Tomo-PIV reconstruction quality by reducing ghost particles, *Meas. Sci. Technol.*, 024010.

[3] Ferenc, J. and Néda, Z., On the size distribution of Poisson Voronoi cells, *Physica A*, **385**, 2007, 518–526.

[4] Garcia, D., A fast all-in-one method for automated post-processing of PIV data, *Exp. Fluids*, **50**, 2011, 1247–1259.

[5] Gualtieri, P., Picano, F. and Casciola, C. M., Anisotropic clustering of inertial particles in homogenous shear flow, *J. Fluid Mech.*, **629**, 2009, 25–39.

[6] Lau, T. C. W. and Nathan, G. J., The influence of Stokes number on the velocity and concentration distributions in particle-laden jets, *J. Fluid Mech.*, **757**, 2014, 432–457.

[7] Lau, T. C. W. and Nathan, G. J., The effect of Stokes number on particle velocity and concentration distributions in a well-characterised, turbulent, co-flowing two-phase jet, *J. Fluid Mech.*, **809**, 2016, 72–110.

[8] Lau, T. C. W. and Nathan, G. J., The influence of Stokes number on particle clustering at the exit of a turbulent jet issuing from a long round pipe, in *Proc. of the 9th Int. Conf. on Multiphase Flow*, Firenze, Italy, 2016.

[9] Lau, T. C. W. and Nathan, G. J., A method for identifying and characterising particle clusters in a two-phase turbulent jet, *Int. J. Multiphase Flow*, **88**, 2017, 191–204.

[10] Lazar, E. A., Mason, J. K., MacPherson, R. D. and Srolovitz, D. J., Statistical topology of three-dimensional Poisson-Voronoï cells and cell boundary networks, *Physical Review E*, **88**, 2013, 063309.

[11] Longmire, E. K. and Eaton, J. K., Structure of a particle-laden round jet, *J. Fluid Mech.*, **236**, 1992, 217–257.

[12] Monchaux, R., Bourgoin, M. and Cartellier, A., Preferential concentration of heavy particles: A Voronoï analysis, *Physics of Fluids*, **22**, 2010, 103304.

[13] Novara, M., Batenburg, K. J. and Scarano, F., Motion tracking-enhanced MART for tomographic PIV, *Meas. Sci. Technol.*, **21**.

[14] Smith, N. L., Nathan, G. J., Zhang, D. K. and Nobes, D. S., The significance of particle clustering in pulverized coal flames, *Proc. of the Comb. Inst.*, **29**, 2002, 797–804.

[15] Westerweel, J. and Scarano, F., Universal outlier detection for PIV data, *Exp. Fluids*, **39**, 2005, 1096–1100.